Developmental remodeling repurposes larval neurons for sexual behaviors in adult *Drosophila*

Julia A. Diamandi, Julia C. Duckhorn, Kara E. Miller, Mason Weinstock, Sofia Leone, Micaela R. Murphy, and Troy R. Shirangi*

Villanova University, Department of Biology, 800 East Lancaster Ave, Villanova, PA 19085

* Correspondence: troy.shirangi@villanova.edu

Summary

Most larval neurons in *Drosophila* are repurposed during metamorphosis for functions in adult life, but their contribution to the neural circuits for sexually dimorphic behaviors is unknown. Here, we identify two interneurons in the nerve cord of adult *Drosophila* females that control ovipositor extrusion, a courtship rejection behavior performed by mated females. We show that these two neurons are present in the nerve cord of larvae as mature, sexually monomorphic interneurons. During pupal development, they acquire the expression of the sexual differentiation gene, *doublesex*, undergo *doublesex*-dependent programmed cell death in males, and are remodeled in females for functions in female mating behavior. Our results demonstrate that the neural circuits for courtship in *Drosophila* are built in part using neurons that are sexually reprogrammed from former sex-shared activities in larval life.

Introduction

Many behaviors of adult animals develop during a period of maturation (*e.g.*, puberty) as the nervous system transforms from its juvenile to adult form[1]. Extensive anatomical changes in the central nervous system occur during this time, including the gain and differentiation of new neurons that compose adult circuits[2]. However, in many animals like insects[3] and worms[4], the adult nervous system is also assembled with reprogrammed neurons that were formerly active in the juvenile.

During *Drosophila* metamorphosis, most neurons of the larval central nervous system are recycled for use in adult circuits[5]. The moonwalker descending neuron, for instance, triggers backward locomotion in crawling larvae and is remodeled during pupal life to regulate backward walking in adult flies[6]. Additionally, several input and output neurons of the larval mushroom body trans-differentiate during metamorphosis and contribute to entirely different circuits in the adult brain[3]. Despite these cases, there are currently no examples of recycled larval neurons that contribute to sexually dimorphic behaviors of adult flies. Indeed,-lineage analyses of adult neurons with sexual identity in *Drosophila* suggest that most are born post-embryonically and contribute exclusively to sexually dimorphic behaviors in adults[7,8].

We previously identified a small sexually dimorphic population of interneurons in the abdominal ganglion of adult flies, the DDAG neurons, that co-express the *tailless*-like orphan nuclear receptor, *dissatisfaction* (*dsf*), and the sex differentiation gene, *doublesex* (*dsx*)[9]. Here, we identify two female-specific DDAG neurons that influence the extrusion of the ovipositor performed by mated females to reject courting males. These two DDAG neurons are born during embryogenesis and exist as segmental homologs of a sexually monomorphic interneuron in the larval abdominal ganglion called A26g. During early pupal life, the A26g neuron at abdominal segments five and six acquire the expression of *dsx*, undergo *dsx*-dependent programmed cell death in males, and are remodeled in females for use in the circuitry for ovipositor extrusion. Our results demonstrate that the neural circuits for sexually dimorphic behaviors in *Drosophila* include sexually reprogrammed neurons with former activities in the juvenile larva of both sexes.

Results

The DDAG neurons are anatomically diverse

Drosophila melanogaster females and males have eleven and three *dsf*- and *dsx*-co-expressing abdominal ganglion (DDAG) neurons, respectively, which contribute to several mating behaviors in both sexes (Figure 1A)[9]. As a first step toward associating specific courtship functions to specific DDAG

52 neurons, we employed a stochastic labeling method to determine the anatomy of individual DDAG neurons in females and males.

54 The DDAG neurons are labeled by a genetic intersectional strategy whereby a Flp recombinase, driven in *dsx*-expressing cells by *dsx*$^{LexA::p65}$ [10], excises a transcriptional stop cassette from an upstream 56 activating sequence (UAS)-regulated *myr::gfp* transgene. Expression of *myr::gfp* is activated in *dsf*-co-expressing cells by the *dsf*^{Gal4} allele[9]. To stochastically label individual DDAG neurons using a similar 58 intersectional strategy, we utilized *FlpSwitch*[11], a Flp recombinase fused to the ligand binding domain of the human Progesterone Receptor (hPR). The activity of the FlpSwitch recombinase is dependent upon 60 the presence of the progesterone mimic, mifepristone. We constructed flies carrying the *dsf*^{Gal4} and *dsx*$^{LexA::p65}$ alleles, a UAS-regulated *FlpSwitch*, and a LexAop-regulated *myr::gfp* transgene containing a 62 transcriptional stop cassette that is conditionally excised by the FlpSwitch recombinase. When these flies were fed food containing mifepristone for a relatively short period of time, single DDAG neurons were 64 often labeled in adult flies. We examined approximately 60 and 20 single cell clones in female and male ventral nerve cords, respectively, and identified five anatomically distinct DDAG subtypes (Figure 1B). 66 One of these subtypes, DDAG_A, is present in both sexes, whereas the DDAG_B–E subtypes are specific to females. All DDAG neuronal subtypes arborize extensively in the abdominal ganglion, whereas the 68 DDAG_C–E neurons also extend an anteriorly projecting branch that innervates thoracic neuropils. We conclude that the DDAG neuronal population consists minimally of five anatomical subtypes. Additional 70 DDAG subtypes may exist that were not labeled in our experiments, and the number of neurons of each subtype is unclear.

72

DDAG_C and DDAG_D neurons contribute to ovipositor extrusion

74 The five DDAG subtypes identified above in females may contribute to different reproductive behaviors. To develop driver lines that target subsets of DDAG neurons, we used CRISPR/Cas9-mediated 76 homology-directed repair to create new alleles of *dsf* that express *LexA::p65*, or the Split-Gal4 hemi-drivers, *p65AD::Zp* and *Zp::GAL4DBD*, in *dsf*-expressing cells. In a search for Split-Gal4 drivers that target 78 subsets of DDAG neurons, we found that intersecting *dsf*$^{p65AD::Zp}$ with the enhancer line, *VT026005-Zp::GDBD*, labeled four female-specific DDAG neurons on the left and right sides of the adult ventral 80 nerve cord (Figure 2A, B). Two cell bodies are located at the posterior tip of the nerve cord and the other two are at the dorsal side of the abdominal ganglion. Labeling of individual neurons by the multicolor 82 Flp-out technique[12] identified the two neurons at the tip as a local interneuron subtype corresponding to DDAG_B, whereas the dorsally located cell bodies are the DDAG_C and DDAG_D neurons (Figure 2C).

The DDAG_C and DDAG_D neurons are segmental homologs (see below) and exhibit some anatomical similarities. Both neurons extend a primary branch off the cell body forming a "ventral arch" that projects across the midline and then anteriorly on the contralateral dorsal side. Unlike the DDAG_D neuron, the DDAG_C neuron extends a dorsally projecting medial branch off the ventral arch that gives rise to arbors within the abdominal ganglion. We were unable to differentiate the two DDAG_B neurons, however they may exhibit subtle anatomical differences that were undetected in our analysis and contribute to female behavior differently.

We asked how the neurons labeled by *dsf*$^{p65AD::Zp}$ ∩ *VT026005-Zp::GDBD* influence female behavior. During courtship, unmated *D. melanogaster* females signal their willingness to mate by opening their vaginal plates and partially exposing their ovipositor, a behavior called "vaginal plate opening," or vpo[13,14]. Mated females, however, reject courting males by fully extruding their ovipositor, which may block copulation or male courtship drive[14,15]. We previously showed that transient photoactivation of all DDAG neurons using the mVenus-tagged, red-light-gated cation channelrhodopsin, *CsChrimson::mVenus*[16], caused unmated females to open their vaginal plates and mated females to extrude their ovipositor[9]. Upon photoactivation, *dsf*$^{p65AD::Zp}$ ∩ *VT026005-Zp::GDBD* > *CsChrimson::mVenus* females fully extruded their ovipositor regardless of their mating status (Figure 2D; Video S1, S2). Extrusion of the ovipositor was penetrant and occurred only during the photoactivation period (Figure 2E), and quantitatively similar behaviors were observed across a range of stimulus intensities (Figure 2G). To confirm that photoactivation of the DDAG_B–D neurons in unmated and mated females triggered an ovipositor extrusion and not an opening of the vaginal plates, we measured the change in abdominal length before and during photoactivation of the DDAG_B–D neurons in unmated and mated females and compared it to the change in abdominal length when all DDAG neurons were photoactivated in unmated and mated females. Optogenetic activation of all DDAG neurons in mated females, which induces ovipositor extrusion, caused a larger change in abdominal length compared to unmated females, which open the vaginal plates[9] (Figure 2F). Photoactivation of the DDAG_B–D neurons in unmated and mated females induced a change in abdominal length more similar to that measured when all DDAG neurons were photoactivated in mated females (Figure 2F).

We next tested whether activity of the DDAG_B–D neurons was required for ovipositor extrusion in mated females. In addition to labeling a subset of female-specific DDAG neurons, the intersection of *dsf*$^{p65AD::Zp}$ and *VT026005-Zp::GDBD* labels several additional neurons in the brain (Figure 2A). To target the DDAG_B–D neurons specifically, we intersected *dsf*$^{p65AD::Zp}$ ∩ *VT026005-Zp::GDBD* with *dsx*$^{LexA::p65}$ (Figure 3A) and used the three-way intersection to suppress the activity of the DDAG_B–D neurons by

116 driving the expression of a GFP-tagged version of the inwardly rectifying K+ channel, *Kir2.1*[17] (Figure 3B).
Unmated females expressing *Kir2.1::gfp* in the DDAG_B–D neurons copulated with males at a rate that
118 was similar to control unmated females (Figure 3C) and opened their vaginal plates during courtship at a
frequency comparable to control females (Figure 3D). However, mated *dsf*$^{p65AD::Zp}$ ∩ *VT026005-Zp::GDBD*
120 ∩ *dsx*$^{LexA::p65}$ > *Kir2.1::gfp* females extruded their ovipositor during courtship with significantly reduced
frequency (Figure 3E) and laid fewer eggs (Figure 3F) compared to controls. Thus, the activity of one or
122 more DDAG subtypes labeled by the *dsf*$^{p65AD::Zp}$ ∩ *VT026005-Zp::GDBD* intersection are necessary for
ovipositor extrusion and egg laying in mated females.

124 To determine the specific DDAG neuronal subtype that influences ovipositor extrusion, we
randomly expressed *CsChrimson::mVenus* in one or more neurons labeled by the *dsf*$^{p65AD::Zp}$ ∩ *VT026005-*
126 *Zp::GDBD* intersection using a Flp-based approach. By stochastically expressing a Flp recombinase under
the control of a heat-inducible promoter, we randomly excised a transcriptional stop cassette from a UAS-
128 regulated *CsChrimson::mVenus* transgene whose expression was driven by *dsf*$^{p65AD::Zp}$ ∩ *VT026005-*
Zp::GDBD. Using this strategy, we generated a population of mosaic females (n=104) that randomly
130 expressed *CsChrimson::mVenus* in one or more of the DDAG neurons labeled by *dsf*$^{p65AD::Zp}$ ∩ *VT026005-*
Zp::GDBD, uni- or bilaterally. Females were tested in an optogenetic activation experiment before their
132 ventral nerve cords were dissected and stained with antibodies to GFP to reveal the identity of DDAG
neurons that expressed the *CsChrimson::mVenus* in each female.

134 All females expressing *CsChrimson::mVenus* bilaterally in the DDAG_C (n=11) or DDAG_D (n=6)
neurons extruded their ovipositor during bouts of photoactivation (Figure 2H, I; Video S3, S4), whereas
136 unilateral activation of the DDAG_C (n=33) or DDAG_D (n=33) neurons caused a change in abdominal
posture with no extrusion of the ovipositor (Figure 2H, Video S5, S6). Since the two DDAG_B neurons
138 labeled by *dsf*$^{p65AD::Zp}$ ∩ *VT026005-Zp::GDBD* are anatomically indistinguishable, we were unable to
identify mosaic females that expressed *CsChrimson::mVenus* specifically in lateral homologs of one
140 DDAG_B neuron. Nevertheless, unilateral activation of the DDAG_B neuron (n=16) failed to evoke any
obvious behavior (Figure 2H, Video S7), and bilateral activation of the DDAG_B neurons did not modify
142 the postural change induced by photoactivation of a single DDAG_C or DDAG_D neuron (Figure 2H,
Video S8). We never obtained mosaic females that expressed *CsChrimson::mVenus* only in a bilateral pair
144 of DDAG_B neurons. Taken together, these results demonstrate that the DDAG_C and DDAG_D neurons
contribute to ovipositor extrusion in mated females. A functional difference between the DDAG_C and
146 DDAG_D were not detected in our experiments. The contribution of the DDAG_B neurons to female
behavior is unclear.

148

The DDAG neurons originate as embryonic-born neurons in the larval ventral nerve cord

150 In the abdominal ganglion of the late larval ventral nerve cord, the *dsf*^{Gal4} allele labels two segmentally repeating bilateral neurons from A1 to A8, and four bilateral neurons at the terminal
152 segments (Figure 4A). The number and gross anatomy of these neurons is similar in female and male larvae, in newly hatched larvae, and in larvae aged 24 and 48 hours after hatching (Figure 4A), indicating
154 that the neurons are born during embryogenesis, and that the expression of the *dsf*^{Gal4} allele is stable through larval life. We posited that a subset of these twenty *dsf*-expressing neurons on each side of the
156 abdominal ganglion of larvae become the DDAG neurons of adult females and males. We tested this by visualizing *dsf*^{Gal4} and *dsx*$^{LexA::p65}$ expression in the abdominal ganglion of pupae staged at several times
158 during pupal development. From 0 to 18 hours after puparium formation (APF), the twenty *dsf*-expressing neurons we observed in the abdominal ganglion of larvae were identifiable in the ventral
160 nerve cord of female and male pupae (Figure 4B, C). By 18 hours APF, approximately eleven of these neurons had gained *dsx*$^{LexA::p65}$ expression in both sexes (Figure 4B, C). In neuromeres A3–A7, one of the
162 two *dsf*-expressing neurons in each hemisegment was labeled by *dsx*$^{LexA::p65}$, and all six *dsf*-expressing neurons in A8 and the terminal segments co-expressed *dsx*$^{LexA::p65}$ (Figure 4B). The gain of *dsx*$^{LexA::p65}$
164 expression in *dsf*-expressing neurons occurred gradually and monomorphically in both sexes from 0 to 18 hours APF, but by 36 hours APF, approximately eight *dsf*^{Gal4} and *dsx*$^{LexA::p65}$ co-expressing neurons were
166 absent in males (Figure 4C). We previously demonstrated that the difference in DDAG neuron number between adult females and males was due to *dsx*-dependent apoptosis in males[9], indicating that the loss
168 of *dsf*^{Gal4} and *dsx*$^{LexA::p65}$ co-expressing neurons in male pupae aged 36 hours APF is due to cell death. At 48 hours APF, approximately eleven and three *dsf*^{Gal4} and *dsx*$^{LexA::p65}$ co-expressing neurons were present in
170 the abdominal ganglion of females and males, respectively, corresponding to the number of DDAG neurons in adults (Figure 4C).

172 To further test that the DDAG neurons are derived from *dsf*-expressing neurons in the abdominal ganglion of larvae, we repeated the Flp-based genetic intersection between *dsf*^{Gal4} and *dsx*$^{LexA::p65}$, but this
174 time, we used *UAS-FlpSwitch* to conditionally activate the recombinase in *dsf*^{Gal4}-expressing cells only during larval life. Larvae were fed mifepristone, causing the FlpSwitch to excise a transcriptional stop
176 cassette from a LexAop-controlled *myr::gfp* transgene in larval cells labeled by the *dsf*^{Gal4}. The *dsx*$^{LexA::p65}$ allele was used to drive the expression of *myr::gfp* in *dsx*-expressing neurons of adults. GFP expression
178 was observed in the DDAG neurons of adults of both sexes (Figure S1), consistent with the notion that the DDAG neurons originate as *dsf*-expressing neurons in the larval abdominal ganglion. We conclude that

180 the entire population of DDAG neurons are embryonic-born *dsf*-expressing neurons that are present in larvae both sexes. During pupal life, approximately eleven *dsf*-expressing neurons in the abdominal
182 ganglion of both sexes gain *dsx* expression (Figure 4B, C), eight of which are subsequently lost in males due to *dsx*-mediated apoptosis[9].

184

Two segmental homologs of the A26g neuron in larvae become the DDAG_C and DDAG_D neurons
186 **of adult females**

We next sought to identify the larval counterparts of specific DDAG neuronal subtypes. We
188 found that the intersection of *dsf*$^{p65AD::Zp}$ and *VT026005-Zp::GDBD* used above to target the DDAG_B–D subtypes labeled a single, bilateral, and segmentally repeating *dsf*-expressing interneuron in segments
190 A4–A6 of the larval abdominal ganglion of both sexes (Figure 5A, B). Stochastic labeling of individual neurons labeled by the Split-Gal4 demonstrated that all three neurons correspond to the A26g
192 interneuron (Figure 5C; J. Truman, personal communication).

The A26g neuron of larvae and the DDAG_C and DDAG_D neurons of adult females display
194 several anatomical similarities. All three neurons have a cell body on the dorsal side of the abdominal ganglion, a ventral arch, and a dorsally-located contralateral branch that projects anteriorly. We therefore
196 hypothesized that two segmental homologs of the A26g neuron labeled in larvae by *dsf*$^{p65AD::Zp}$ ∩ *VT026005-Zp::GDBD* metamorphose into the DDAG_C and DDAG_D neurons of adults. To test this, we
198 first visualized the A26g neurons labeled by *dsf*$^{p65AD::Zp}$ ∩ *VT026005-Zp::GDBD* over the course of pupal development in females and probed DSX-F protein expression. At the onset of pupariation, the A26g
200 neurons at A4–A6 were labeled by *dsf*$^{p65AD::Zp}$ ∩ *VT026005-Zp::GDBD* but none of them co-expressed DSX-F (Figure 5D). By 24 hours APF, however, the A26g neuron at A5 and A6, but not A4, had gained DSX-F
202 expression (Figure 5E). Two additional neurons, one at A7 and one at A8, were labeled by the Split-Gal4 and both were also marked by DSX-F (Figure 5E). All five GFP+ neurons per side were present in the
204 abdominal ganglion at 48 hours APF, but the morphology of DSX-F-expressing A5 and A6 neurons had transformed to the likeness of the DDAG_D and DDAG_C neurons, respectively, and the DSX-F+ A7 and
206 A8 neurons appeared like the DDAG_B neurons (Figure 5F). Additionally, the cell bodies of the A5 and A6 neurons were positioned on the dorsal side of the abdominal ganglion where the soma of the
208 DDAG_D and DDAG_C neurons are normally located, and the A7 and A8 cell bodies were at the tip of the nerve cord, where the DDAG_B neurons are found. By adulthood, the DSX-F-non-expressing A26g
210 neuron at A4 had disappeared (Figure 5G). These data suggest that the A26g neuron at segments A5 and A6 of the larval abdominal ganglion in females transform into the DDAG_D and DDAG_C neurons,

212 respectively. The DDAG_B neurons are derived from *dsf*-expressing neurons at A7 and A8 that become marked by *dsf*$^{p65AD::Zp}$ ∩ *VT026005-Zp::GDBD* during pupal development prior to 24 hours APF.

214 To confirm that the A26g neurons in larvae become the DDAG_C and DDAG_D neurons, we repeated the FlpSwitch-based genetic intersection we described above but between *dsx*$^{LexA::p65}$ and

216 *dsf*$^{p65AD::Zp}$ ∩ *VT026005-Zp::GDBD*. The Split-Gal4 drove the expression of a UAS-*FlpSwitch* in the A26g neurons and larvae were fed mifepristone to activate the FlpSwitch during larval life, which excised a

218 transcriptional stop cassette from a LexAop-controlled *myr::gfp* transgene driven by *dsx*$^{LexA::p65}$. The DDAG_C and DDAG_D neurons of adult females were labeled by GFP (Figure 5H), further confirming

220 that the DDAG_C and DDAG_D neurons are indeed derived from two segmental homologs of the A26g neurons in larvae.

222

DSF and DSX-M regulate the survival of the DDAG_C and DDAG_D neurons

224 We previously showed that DSF activity is required for the survival of a subset of DDAG neurons in females, whereas DSX-M promotes the cell death of female-specific DDAG neurons in males[9]. We

226 sought to determine how DSF and DSX contribute to the development of the DDAG_C and DDAG_D neurons, specifically. The *dsf*$^{p65AD::Zp}$ ∩ *VT026005-Zp::GDBD* intersection was used to visualize the

228 DDAG_C and DDAG_D neurons while driving the expression of a validated UAS-regulated short hairpin/miRNA (ShmiR) targeting *dsf* or *dsx* transcripts. *Dsx* transcripts are sex-specifically spliced and

230 translated to produce female- and male-specific isoforms of DSX proteins. Knock-down of *dsx* transcripts in females did not cause any obvious change in DDAG_C or DDAG_D anatomy (Figure S2A, B), whereas

232 depletion of male-specific *dsx* transcripts caused a gain of DDAG_C and DDAG_D neurons with an arborization pattern like that of wild-type females (Figure S2A′, B′). Female-specific DDAG neurons can

234 be resurrected in males by the ectopic expression of the cell death inhibitor, P35[9], suggesting that the gain of the DDAG_C and DDAG_D neurons in *dsf*$^{p65AD::Zp}$ ∩ *VT026005-Zp::GDBD* > *UAS-dsx_ShmiR* males is

236 due to loss of cell death. Optogenetic activation of the resurrected DDAG_C and DDAG_D neurons in *dsf*$^{p65AD::Zp}$ ∩ *VT026005-Zp::GDBD* > *UAS-dsx_ShmiR* males induced an extrusion of the male's terminalia

238 (Video S9), a behavior reminiscent of ovipositor extrusion in mated females. Consistent with the absence of an anatomical phenotype in the DDAG_C and DDAG_D neurons, *dsf*$^{p65AD::Zp}$ ∩ *VT026005-Zp::GDBD* >

240 *UAS-dsx_ShmiR* females extruded their ovipositor upon photoactivation of the neurons labeled by the Split-Gal4 (Figure S2G, Video S10).

242 In contrast, the DDAG_C and DDAG_D neurons were lost in *dsf*$^{p65AD::Zp}$ ∩ *VT026005-Zp::GDBD* > *UAS-dsf_ShmiR* females (Figure S2A, C) and in females carrying loss-of-function mutations in *dsf* (Figure

244 S2D, E). When *dsf*$^{p65AD::Zp}$ ∩ *VT026005-Zp::GDBD* was used to drive the expression of *UAS-dsf_ShmiR* and *UAS-CsChrimson::mVenus*, females failed to extrude their ovipositor during bouts of photoactivation
246 (Figure S2G, Video S11). To confirm that the loss of the DDAG_C and DDAG_D neurons in *dsf* mutant females was due to cell death, we used *dsf*^{Gal4} to drive the expression of *UAS-P35*. Indeed, blockage of cell
248 death by ectopic expression of P35 in *dsf*-expressing neurons of *dsf* mutant females rescued the DDAG_C and DDAG_D neurons (Figure S2D–F). The rescued DDAG_C and DDAG_D neurons appear to lack
250 contralateral ascending projections, suggesting that *dsf* may contribute to neuronal development beyond acting as a pro-survival factor. Knock-down of *dsf* transcripts in *dsf*$^{p65AD::Zp}$ ∩ *VT026005-Zp::GDBD* > *UAS-*
252 *dsf_ShmiR* males had no effect upon DDAG_C and DDAG_D development (Figure S2A′, C′). Taken together, these data suggest that DSF promotes the survival of the DDAG_C and DDAG_D neurons in
254 females, whereas DSX-M promotes their cell death in males. Knock-down of *dsf* transcripts in *dsf*$^{p65AD::Zp}$ ∩ *VT026005-Zp::GDBD* > *UAS-dsf_ShmiR* larvae had no obvious effect upon the development of the A26g
256 neurons (Figure S2H), suggesting that DSF promotes the survival of the DDAG_C and DDAG_D neurons during pupal development.
258

Discussion

260 Many neurons of the *Drosophila* larval nervous system persist through development and contribute to adult neural circuits, yet their contribution to sexually dimorphic adult behaviors is unclear.
262 In this paper, we address this gap with two key findings: First, we identify two interneurons in the abdominal ganglion of adult females, the DDAG_C and DDAG_D neurons, that contribute to ovipositor
264 extrusion, a behavior performed primarily by mated and mature females to reject courting males. The neural circuitry that mediates ovipositor extrusion in mated females has been partially delineated
266 recently[15]. In response to the male's song, *dsx*-expressing pC2l neurons activate a descending neuron called DNp13 that triggers the motor circuits in the abdominal ganglion for ovipositor extrusion[15].
268 Interestingly, the ability of DNp13 to induce ovipositor extrusion in mated but not unmated females depends upon mechanosensory input during ovulation[15]. The DDAG_C/D neurons may function
270 downstream of DNp13 and ovulation-sensing mechanosensory neurons, perhaps integrating their inputs, but upstream of motor circuits for ovipositor extrusion.

272 Second, we find that the DDAG_C/D neurons are present in the larval abdominal ganglion as mature sexually monomorphic neurons corresponding to two segmental homologs of the A26g neuron.
274 The function of A26g in larvae is currently unknown. During metamorphosis, the A26g neurons at segments A5 and A6 acquire *dsx* expression in both sexes and are then remodeled in females to become

276 the DDAG_D and DDAG_C neurons, respectively. In males, expression of DSX-M promotes programmed cell death of the A26g neurons during pupal life[9], whereas DSF activity is necessary for the
278 survival the A26g neurons in females. The mechanism by which DSF and DSX-M regulate A26g apoptosis is unclear. One possibility is that DSX-M antagonizes DSF function in males, thereby allowing the
280 neurons to die during pupal life.

Our results demonstrate that the neural circuits for courtship behavior in *Drosophila* are
282 constructed in part from sex-non-specific larval neurons that are sexually reprogrammed during metamorphosis for functions in adults (Figure 6). Similar observations have been made in *C. elegans*
284 where sex-specific patterns of synaptic connectivity in adults develop from neurons in juvenile worms with sexually monomorphic connections[18]. How much of the circuitry for dimorphic courtship behaviors
286 in flies is built from reprogrammed larval neurons? Lineage analyses of neurons with sexual identity in the adult brain and thoracic ganglia have shown that most, if not all, are born during post-embryonic
288 neurogenesis and function only in adults[7,8]. However, this may differ in the abdominal nervous system. The abdominal ganglion of adult flies is largely specialized for functions in reproduction, and indeed the
290 majority of *dsx*-expressing neurons are located there[19–21]. Some of these neurons are specific to adults and are born during larval and pupal life from two terminal abdominal neuroblasts (*i.e.*, neural stem cells)
292 with sex-specific patterns of neurogenesis[22–24]. But many others, like the DDAG neurons, are likely to be derived from embryonic lineages. In contrast to the brain and thoracic nervous system, the vast majority
294 of neuroblasts in the abdominal neuromeres (*e.g.*, A2–A8) finish producing neurons by the end of embryonic life and add very few adult-specific neurons[22]. The contribution of remodeled larval neurons
296 to the circuits for sexually dimorphic behaviors may thus be relatively greater in the abdominal ganglion than in other regions of the fly nervous system.

298 Insect neurons exhibit impressive plasticity as the central nervous system metamorphoses from its larval to adult form. Some larval neurons undergo programmed cell death, but most persist through
300 pupal life to contribute to adult circuits[5]. Larval neurons that persist either remodel their axonal and dendritic arbors to regulate similar processes in adults[3,6,25–29] or trans-differentiate to obtain altogether
302 different functions[3,30]. Courtship and neuronal sexual identity are specific to adults, suggesting that the A26g-to-DDAG_C/D transformation may be a case of trans-differentiation. How the A26g neurons
304 acquire sexual identity and become repurposed during metamorphosis may provide a system to study the regulatory mechanisms underlying developmental reprogramming of the nervous system.
306

308 **Methods**

Fly stocks. Drosophila melanogaster stocks were maintained on standard cornmeal and molasses food at
310 25ºC and 50% humidity in a 12-hr light/dark cycle unless otherwise noted. Fly stocks used in this study
include: *Canton S*, w^{1118}, $dsx^{LexA::p65}$/*TM6B*, dsf^{Gal4}/*CyO*, *pJFRC29-10XUAS-IVS-myr::GFP-p10* (attP2), *pJFRC12-*
312 *10XUAS-IVS-myr::GFP* (attP2), *pJFRC79-8XLexAop-2-FlpL* (attP40), *pJFRC41-10XUAS-FRT-STOP-FRT-*
myr::gfp (su(Hw)attP1), *pJFRC108-20XUAS-IVS-hPR-Flp-p10* (attP2), *pJFRC40-13XLexAop-FRT-STOP-FRT-*
314 *myr::gfp* (attP40), *VT026005-Zp::GDBD* (attP2), *pJFRC56-10XUAS-FRT-STOP-FRT-kir2.1::gfp* (attP2),
pBPhsFlp2::PEST (attP3), *pJFRC201-10XUAS-FRT-STOP-FRT-myr::smGFP-HA (VK0005), pJFRC240-*
316 *10XUAS-FRT>STOP>FRTmyr::smGFP-V5-THS-10XUAS-FRT>STOP>FRT-myr::smGFP-FLAG* (su(Hw)
attP1), *20XUAS-FRT>STOP>FRT-CsChrimson::mVenus* (VK5), *UAS-P35.BH1, UAS-dsf_ShmiR* (attP2), and
318 *UAS-dsx_ShmiR* (attP2). $dsf^{p65AD::Zp}$, $dsf^{Zp::GDBD}$, and $dsf^{LexA::p65}$ alleles were generated using the same strategy
as that used to build the dsf^{Gal4} allele[9] except the Gal4 sequence in the donor construct was replaced with
320 sequences encoding *p65AD::Zp*, *Zp::GDBD*, or *LexA::p65*.

322 *Immunohistochemistry.* Nervous systems were dissected in 1X phosphate-buffered saline (PBS), fixed in 4%
paraformaldehyde in PBS for 35 minutes, then rinsed and washed in PBT (PBS with 1% Triton X-100). If a
324 blocking step was performed, nervous systems were incubated in 5% normal goat serum or 5% normal
donkey serum in PBT for 30 minutes. Tissues were then incubated with primary antibodies diluted in
326 PBT or PBT with block overnight at 4°C. The next day, three washes were performed over the course of
several hours before nervous systems were incubated in secondary antibodies diluted in PBT or PBT with
328 block overnight at 4°C. Tissues were then washed three times over the course of several hours and placed
on cover slips coated in poly-lysine, dehydrated in an increasing ethanol concentration series, and cleared
330 in a xylene series. Nervous systems were mounted onto slides using DPX mounting medium and imaged
on a Leica TCS SP8 Confocal Microscope at 40X magnification. For MultiColor FlpOut experiments, vials
332 containing larvae aged between first and second instars (or 3–4-day old adults) were placed in a 37°C
water bath for 1–10 minutes then dissected 2 days later. To stochastically label the DDAG neurons, male
334 and female adults (deprived of food overnight) were placed in vials with food containing 100mM
mifepristone (RU-486; Sigma 475838-50MG) for 2 hours and kept in darkness. Flies were then transferred
336 back to vials containing untreated food for 3 days before their VNCs were dissected for staining. For
immortalization experiments using mifepristone, three days after crosses were set-up on normal food, 60
338 μL of 100mM RU-486 was added directly to the food and larvae were raised in darkness on RU-486-
treated food until pupariation. Pupae were collected and transferred to vials containing untreated food

340 before eclosure. Control groups were also kept in darkness but were treated with 60 μL of ethanol instead of RU-486. Adult nervous systems were dissected in PBS. The following primary antibodies were used:
342 rabbit anti-GFP (Invitrogen #A11122; 1:1000), rat anti-DN-cadherin (DN-Ex#8, Developmental Studies Hybridoma Bank; 1:50), anti-DSX-F (1:200)[31], mouse anti-HA.11 (BioLegend #MMS-101P; 1:250), and rat
344 anti-FLAG (Novus Biologicals #NBP1-06712; 1:200). The following secondary antibodies were used: Fluorescein (FITC) conjugated donkey anti-rabbit (Jackson ImmunoResearch #711-095-152; 1:500), AF-647
346 goat anti-rat (Invitrogen #A21247; 1:500), AF-568 donkey anti-rat (Invitrogen #A78946; 1:500), AF-647 donkey anti-mouse (Invitrogen #A31571; 1:500), AF-488 goat anti-mouse (Invitrogen #A32723), AF-647
348 goat anti-rat (Invitrogen #A21247; 1:500).

350 *Optogenetic assays*. Unmated females used in optogenetic assays were raised in darkness and on food containing 0.2mM all-trans-retinal (sigma-Aldrich #R2500) and were incubated at 25°C and ~50%
352 humidity. Once collected, unmated females were grouped in vials consisting of 15–20 flies for 8–12 days before testing. Flies were anesthetized on ice for ~2 minutes, decapitated under low-intensity light, and
354 were given 15–20 minutes to recover before being transferred to individual behavioral chambers (diameter: 10 mm, height: 3 mm). A FLIR Blackfly S USB3, BFS-U3-31S4M-C camera with a 800 nm long-
356 pass filter (Thorlabs, FEL0800) was used to record optogenetic videos in SpinView. Upon testing, chambers were placed on top of an LED panel with continuous infrared (850 nm) light and recurring
358 photoactivating red (635 nm) light using an Arduino script. To measure change in abdominal length before and during vaginal plate opening or ovipositor extrusion, a ruler (cm/mm) was included in the
360 frame to set the scale. The change in abdominal length was calculated as the difference in the abdominal length from the base of the scutellum to the tip of the abdomen before and during photoactivation.
362 Behavior indices were measured by calculating the average fraction of time spent preforming the behavior during the first three 15-second lights-on periods and the first three 45-second light-off periods.
364 For stochastic optogenetic activation, unmated females carrying *hs-Flp*, *UAS-frt.stop-CsChrimson::mVenus*, and the Split-Gal4 were reared on retinal-containing food, grouped in vials consisting of 15–20 flies, and
366 aged for ~3 days before being placed in a 37°C water bath for periods ranging from 20–60 minutes. Females were then transferred to new vials containing retinal food and aged for an additional 5 days
368 before being tested in an optogenetic activation experiment as described above. Following optogenetics, the VNC of each female was dissected and placed singly in wells of a 60-well mini tray (Fischer Scientific
370 #12-565-155) for staining. Each VNC was subsequently mapped to the female in the optogenetics experiment from which the VNC was obtained.

372

Behavioral assays. Unmated females and males were collected were under CO_2 and aged for 7–10 days in a
374 12-hour light/dark cycle and incubated at 25°C and ~50% humidity. Unmated females were group-housed in vials consisting of 15–20 flies, and *Canton S* males were individually housed. Courtship assays were
376 done within the first two hours of the subjective day. Unmated females and *Canton S* males were transferred to individual behavioral chambers (diameter: 10 mm, height: 3 mm) and recorded for 30
378 minutes using a Sony Vixia HFR700 video camera at 25°C under white light. For experiments using mated females, unmated females were housed with males for 24 hours, anesthetized on ice for ~2
380 minutes, and mated females were collected into a new vial and given 30 minutes to recover. Mated females and *Canton S* males were loaded to chambers and recorded as described above. Courtship index
382 was measured as the total time the male preformed courtship behaviors divided by the total recording time. Courtship index was measured as the total time the male performed courtship behaviors divided by
384 the observation time which was usually about 5 minutes. Vaginal plate opening (vpo) and ovipositor extrusion (oe) frequency was measured as the total number of times a female performed a vpo or oe in a
386 6-min period of active male courtship. Egg laying was measured by allowing females to mate with males before transferring them to individual vials to for 24 hours. The total number of eggs laid in 24 hours by
388 each female was then counted.

390 **Acknowledgements**

We thank J. Truman (University of Washington) for identifying the A26g neuron and suggesting driver
392 lines to target them in larvae; J. Cande and D. Stern (HHMI) for contributing *dsf* alleles; Y. Ding (University of Pennsylvania), J. Lillvis (HHMI), and E. Preger-Ben Noon (Technion) for helpful
394 discussions and comments on the manuscript; and A. McStravog for administrative assistance. T.R.S. is supported by the National Science Foundation (IOS-1845673).

396

Figure Legends

398 **Figure 1. The DDAG neurons are anatomically diverse.** (A) Confocal images of ventral nerve cords (VNCs) from $dsf^{Gal4} \cap dsx^{LexA::p65} > myr::gfp$ males and females. GFP-expressing neurons are labeled in black
400 and DNCad (neuropil) is shown in light gray. (B) Confocal images of individual DDAG neurons from dsf^{Gal4}/*LexAop-frt.stop-myr::gfp*; $dsx^{LexA::p65}$/*UAS-hPR::Flp* males and females fed food containing
402 mifepristone for about two hours during adulthood. A total of one and five DDAG subtypes were identified in males and females, respectively. Coronal and sagittal views of each neuron is shown.

404

Figure 2. The DDAG_C and DDAG_D neurons contribute to ovipositor extrusion in unmated and
406 **mated females.** (A and B) Confocal images of brains and VNCs from *dsf*$^{p65AD::Zp}$ ∩ *VT026005-ZP::GDBD* > *CsChrimson::mVenus* (A) females and (B) males probed with antibodies to GFP. *CsChrimson::mVenus*-
408 expressing neurons are labeled in black and DNCad (neuropil) is shown in light gray. (C) Confocal images of individual DDAG_B, DDAG_C, and DDAG_D neurons from *dsf*$^{p65AD::Zp}$ ∩ *VT026005-ZP::GDBD*
410 > multicolor flp-out females. Arrows point to the ventral arch of the DDAG_C and DDAG_D neurons. (D) Still-frame images of decapitated *dsf*$^{p65AD::Zp}$ ∩ *VT026005-ZP::GDBD* > *CsChrimson::mVenus* unmated and
412 mated females before (left) and during (right) illumination with 10.5 μW/mm^2 of red light to activate DDAG_B–D neurons. In both cases, photoactivation results in ovipositor extrusion. (E) Fraction of time
414 unmated and mated females open their vaginal plates or extrude their ovipositor during a 15-second bout of photoactivation (*i.e.*, vpo/oe index) of the entire DDAG population (left) or the DDAG subtypes labeled
416 by *dsf*$^{p65AD::Zp}$ ∩ *VT026005-ZP::GDBD* (right). (F) Photoactivation of the entire DDAG population in unmated and mated females induces a change in abdominal length associated with vaginal plate opening
418 and ovipositor extrusion, respectively[9]. Photoactivation of the DDAG_B–D subtypes in unmated and mated females induces a change in abdominal length comparable to that observed in ovipositor
420 extrusion. The change in abdominal when an unmated or mated Canton S female performs vaginal plate opening or ovipositor extrusion is shown for comparison. (G) The change in abdominal length upon
422 photoactivation of *dsf*$^{p65AD::Zp}$ ∩ *VT026005-ZP::GDBD* > *CsChrimson::mVenus* in unmated and mated females is similar across increasing light intensities. (H) Stacked bar graph of behaviors performed by mosaic
424 *dsf*$^{p65AD::Zp}$ ∩ *VT026005-ZP::GDBD* unmated females where *CsChrimson::mVenus* was not expressed or was expressed randomly in DDAG_B, _C, or _D neurons uni- or bilaterally via expression of a heat-inducible
426 Flp recombinase. (I) Still-frame images of mosaic *dsf*$^{p65AD::Zp}$ ∩ *VT026005-ZP::GDBD* unmated females before (left) and during (right) illumination with 10.5 μW/mm^2 of red light to activate DDAG_C or
428 DDAG_D neurons bilaterally and specifically. In both cases, photoactivation results in ovipositor extrusion. (E–G) show individual points, mean, and SD. A one-way ANOVA Turkey-Kramer test for
430 multiple comparisons was used to measure significance (P<0.05). Same letter indicates no significant difference (P>0.05).

432

Figure 3. Activity of neurons labeled by *dsf*$^{p65AD::Zp}$ ∩ *VT026005-ZP::GDBD* is necessary for ovipositor
434 **extrusion and egg laying in mated females.** (A) Confocal images of the brain and VNC from *dsf*$^{p65AD::Zp}$ ∩ *VT026005-ZP::GDBD* ∩ *dsx*$^{LexA::p65}$ > *myr::gfp* females. GFP-expressing neurons are labeled in black and

436 DNCad (neuropil) is shown in light gray. (B) Confocal image of a VNC from *dsf*$^{p65AD::Zp}$ ∩ *VT026005-ZP::GDBD* ∩ *dsx*$^{LexA::p65}$ > *kir2.1::gfp* females. GFP-expressing neurons are labeled in black and DNCad
438 (neuropil) is shown in light gray. (C, D) Unmated females with inhibited DDAG_B–D neurons using *kir 2.1::gfp* are similarly receptive to male courtship relative to two control genotypes. (C) Fraction of
440 unmated females that mated with a naïve *Canton S* male over a 30-min period. Significance (P<0.05) was measured using a Logrank test. (D) Number of times an unmated female opened her vaginal plates per
442 minute of active courtship from a naïve *Canton S* male. (E, F) Ovipositor extrusion and egg laying are reduced in mated females with inhibited DDAG_B–D. (E) Number of times a mated female extruded her
444 ovipositor per minute of active courtship from a naïve *Canton S* male. (F) Number of eggs laid by a mated female 24-hr after mating. (D–F) show individual points, mean, and SD. A one-way ANOVA Turkey-
446 Kramer test for multiple comparisons was used to measure significance (P<0.05). Same letter indicates no significant difference (P>0.05).

448

Figure 4. The DDAG neurons originate as embryonic-born *dsf*-expressing interneurons in the
450 **abdominal ganglion of larvae.** (A) Confocal images of central nervous systems (CNSs) from *dsf*^{Gal4} > *myr::gfp* larvae at various hours post-hatching (hph). GFP-expressing neurons are labeled in black and
452 DNCad (neuropil) is shown in light gray. *dsf*^{Gal4} labels 20 interneurons per side in the abdominal ganglion of female and male larvae. These neurons are observed in newly hatched larvae and are thus born during
454 embryogenesis. The sex of the larvae at 0–2 and 24–26 hph was not determined. (B) A subset of *dsf*-expressing neurons in the abdominal ganglion of larvae acquire *dsx* expression during pupal life. (left)
456 Confocal images of the VNC from *dsf*^{Gal4} > *myr::rfp*, *dsx*$^{LexA::p65}$ > *myr::gfp* female and male pupae at 18 hours after puparium formation (apf). RFP-expressing neurons are labeled in green, GFP-expressing neurons
458 are in magenta, and DNCad (neuropil) is shown in blue. (right) *dsf*^{Gal4}-expressing neurons at each abdominal neuromere are shown. Neurons that co-express *dsx*$^{LexA::p65}$ are labeled with an asterisk. From
460 A3–A7, one of two *dsf*^{Gal4}-expressing neurons are also positive for *dsx*$^{LexA::p65}$, whereas all *dsf*^{Gal4}-expressing neurons posterior to A7 co-express *dsx*$^{LexA::p65}$. (C) The number of *dsf*^{Gal4}-expressing neurons (circles) and
462 *dsf*^{Gal4}-, *dsx*$^{LexA::p65}$-co-expressing (*i.e.*, DDAG) neurons (diamonds) per side in the abdominal ganglion of females (black) and males (magenta). From 0–18 hours apf, the number of *dsf*^{Gal4}-expressing neurons
464 remains at ~20 in both sexes while the number of DDAG neurons gradually increases to ~11 neurons in both sexes. Between 18–48 hours apf, ~8 DDAG neurons gradually disappear in males but not females
466 leaving a total of 11 and 3 DDAG neurons in females and males, respectively. Individual points, mean, and SD are shown.

468

Figure 5. Two A26g neurons in the larval abdominal ganglion become the DDAG_C and DDAG_D
470 **neurons of adult females.** (A, B) Confocal images of larval CNSs from *dsf*$^{p65AD::Zp}$ ∩ *VT026005-ZP::GDBD* > *myr::gfp* (A) females and (B) males. GFP-expressing neurons are labeled in black and DNCad (neuropil) is
472 shown in light gray. The A26g neuron is labeled in segments A4–A6. (C) A confocal image of a single A26g neuron at A4 or A5 using the multicolor Flp-out technique. Coronal and sagittal views are shown.
474 (D–G) Confocal images of the abdominal ganglion at various time points after puparium formation (apf) from *dsf*$^{p65AD::Zp}$ ∩ *VT026005-ZP::GDBD* > *myr::gfp* females. GFP-expressing neurons are labeled in green
476 and DSX-F-expressing neurons are labeled in magenta. (D) At 0 hours apf, the A26g neuron at A4–A6 is labeled by GFP, but none of the neurons express DSX-F. (E) At 24 hours apf, the A26g neuron at A5 and
478 A6 express DSX-F. Two additional neurons at A7 and A8 are labeled by *dsf*$^{p65AD::Zp}$ ∩ *VT026005-ZP::GDBD*, both of which express DSX-F. (F) By 48 hours apf, the GFP+, DSX-F+ neurons at A5 and A6 are
480 anatomically similar to the DDAG_D and DDAG_C neurons, respectively. The GFP+, DSX-F+ neurons at A7 and A8 are anatomically similar to the DDAG_B neuron. (G) By adulthood, only neurons at A5
482 (DDAG_D), A6 (DDAG_C), A7, and A8 (DDAG_B) are labeled by GFP and DSX-F. (H) Confocal images of posterior VNCs from *dsf*$^{p65AD::Zp}$ ∩ *VT026005-ZP::GDBD* > *UAS-hPR::Flp*, *dsx*^{LexAp65} > *LexAop2-frt.stop-*
484 *myr::gfp* adult females fed ethanol- or mifepristone-containing food during larval life. GFP-expressing neurons are labeled in black and DNCad (neuropil) is shown in light gray. Expression of GFP in the
486 DDAG_C and DDAG_D neurons of adults indicates that the cells existed among the *dsf*$^{p65AD::Zp}$ ∩ *VT026005-ZP::GDBD*-expressing neurons in the larval abdominal ganglion. The DDAG_B neurons were
488 also labeled in these experiments; however this was likely due to the presence of residual mifepristone after pupariation and the labeling of the A7 and A8 DDAG_B neurons by the Split-Gal4 during the first 24
490 hours of pupal life.

492 **Figure 6. A26g neurons in larvae become the DDAG_D and DDAG_C neurons in females but undergo *dsx*-dependent cell death in males.** A model summarizing the results described in this paper.

494

Figure S1 related to Figure 4. Confocal images of VNCs from *dsf*^{Gal4} > *UAS-hPR::Flp*, *dsx*$^{LexA::p65}$ > *LexAop2-*
496 *frt.stop-myr::gfp* females and males fed ethanol- or mifepristone-containing food during larval life. GFP-expressing neurons are labeled in black and DNCad (neuropil) is shown in light gray. Scale bar = 50 μm.

498

Figure S2 related to Figure 5. Confocal images of posterior VNCs from *dsf*$^{p65AD::Zp}$ ∩ *VT026005-Zp::GDBD* > *myr::gfp* females (A–C) and males (A′–C′). Control flies (A, A′), and flies carrying *UAS-dsx_ShmiR* (B, B′) or *UAS-dsf_ShmiR* (C, C′) transgenes are shown. (D–F) Confocal images of posterior VNCs from *dsf*^{Gal4} ∩ *dsx*$^{LexA::p65}$ > *myr::gfp* females. Control flies (D) and flies carrying *UAS-dsf_ShmiR* (E) or *UAS-dsf_ShmiR* + *UAS-P35* transgenes are shown. Coronal and sagittal views of each VNC is shown. Arrows point to the ventral arch of DDAG_C/D neurons. Asterisks note the location of dorsal cell bodies corresponding to the DDAG_C/D neurons. GFP-expressing neurons are shown in black and NCad (neuropil) is shown in gray. (G) Fraction of time *dsf*$^{p65AD::Zp}$ ∩ *VT026005-Zp::GDBD* unmated females extrude their ovipositor during a 15-sec bout of photoactivation (*i.e.*, oe index). Control females and females carrying *UAS-dsx_ShmiR* or *UAS-dsf_ShmiR* transgenes are shown. Individual points, mean, and SD are shown. A one-way ANOVA Turkey-Kramer test for multiple comparisons was used to measure significance (P<0.05). Same letter indicates no significant difference. (H) Confocal images of the VNC from *dsf*$^{p65AD::Zp}$ ∩ *VT026005-Zp::GDBD* > *myr::gfp* larvae. Control larvae and larvae carrying a *UAS-dsf_ShmiR* transgene are shown.

Video S1. Optogenetic activation of the DDAG_B–D neurons in unmated females.

Video S2. Optogenetic activation of the DDAG_B–D neurons in mated females.

Video S3. Bilateral optogenetic activation of the DDAG_C neurons in unmated females.

Video S4. Bilateral optogenetic activation of the DDAG_D neurons in unmated females.

Video S5. Unilateral optogenetic activation of a DDAG_C neuron in unmated females.

Video S6. Unilateral optogenetic activation of a DDAG_D neuron in unmated females.

Video S7. Unilateral optogenetic activation of a DDAG_B neuron in unmated females.

Video S8. Bilateral optogenetic activation of the DDAG_B neurons in unmated females.

Video S9. Optogenetic activation of a *dsf*$^{p65AD::Zp}$ ∩ *VT026005-Zp::GDBD* > *CsChrimson::mVenus* male with depleted *dsx* transcripts.

Video S10. Optogenetic activation of a *dsf*$^{p65AD::Zp}$ ∩ *VT026005-Zp::GDBD* > *CsChrimson::mVenus* unmated female with depleted *dsx* transcripts.

Video S11. Optogenetic activation of a *dsf*$^{p65AD::Zp}$ ∩ *VT026005-Zp::GDBD* > *CsChrimson::mVenus* unmated female with depleted *dsf* transcripts.

References

1. Sisk, C.L., and Zehr, J.L. (2005). Pubertal hormones organize the adolescent brain and behavior. Front Neuroendocrinol *26*, 163–174. 10.1016/j.yfrne.2005.10.003.

2. Ahmed, E.I., Zehr, J.L., Schulz, K.M., Lorenz, B.H., DonCarlos, L.L., and Sisk, C.L. (2008). Pubertal hormones modulate the addition of new cells to sexually dimorphic brain regions. Nat Neurosci *11*, 995–997. 10.1038/nn.2178.

3. Truman, J.W., Price, J., Miyares, R.L., and Lee, T. (2023). Metamorphosis of memory circuits in Drosophila reveals a strategy for evolving a larval brain. Elife *12*, e80594. 10.7554/eLife.80594.

4. Witvliet, D., Mulcahy, B., Mitchell, J.K., Meirovitch, Y., Berger, D.R., Wu, Y., Liu, Y., Koh, W.X., Parvathala, R., Holmyard, D., et al. (2021). Connectomes across development reveal principles of brain maturation. Nature *596*, 257–261. 10.1038/s41586-021-03778-8.

5. Truman, J.W., and Riddiford, L.M. (2023). Drosophila postembryonic nervous system development: a model for the endocrine control of development. Genetics *223*, iyac184. 10.1093/genetics/iyac184.

6. Carreira-Rosario, A., Zarin, A.A., Clark, M.Q., Manning, L., Fetter, R.D., Cardona, A., and Doe, C.Q. (2018). MDN brain descending neurons coordinately activate backward and inhibit forward locomotion. Elife *7*, e38554. 10.7554/eLife.38554.

7. Cachero, S., Ostrovsky, A.D., Yu, J.Y., Dickson, B.J., and Jefferis, G.S.X.E. (2010). Sexual dimorphism in the fly brain. Curr Biol *20*, 1589–1601. 10.1016/j.cub.2010.07.045.

8. Ren, Q., Awasaki, T., Huang, Y.-F., Liu, Z., and Lee, T. (2016). Cell Class-Lineage Analysis Reveals Sexually Dimorphic Lineage Compositions in the Drosophila Brain. Curr Biol *26*, 2583–2593. 10.1016/j.cub.2016.07.086.

9. Duckhorn, J.C., Cande, J., Metkus, M.C., Song, H., Altamirano, S., Stern, D.L., and Shirangi, T.R. (2022). Regulation of Drosophila courtship behavior by the Tlx/tailless-like nuclear receptor, dissatisfaction. Curr Biol *32*, 1703-1714.e3. 10.1016/j.cub.2022.02.031.

10. Pan, Y., Robinett, C.C., and Baker, B.S. (2011). Turning males on: activation of male courtship behavior in Drosophila melanogaster. PLoS One *6*, e21144. 10.1371/journal.pone.0021144.

11. Harris, R.M., Pfeiffer, B.D., Rubin, G.M., and Truman, J.W. (2015). Neuron hemilineages provide the functional ground plan for the Drosophila ventral nervous system. Elife *4*, e04493. 10.7554/eLife.04493.

12. Nern, A., Pfeiffer, B.D., and Rubin, G.M. (2015). Optimized tools for multicolor stochastic labeling reveal diverse stereotyped cell arrangements in the fly visual system. Proc Natl Acad Sci U S A *112*, E2967-2976. 10.1073/pnas.1506763112.

13. Wang, K., Wang, F., Forknall, N., Yang, T., Patrick, C., Parekh, R., and Dickson, B.J. (2021). Neural circuit mechanisms of sexual receptivity in Drosophila females. Nature *589*, 577–581. 10.1038/s41586-020-2972-7.

14. Mezzera, C., Brotas, M., Gaspar, M., Pavlou, H.J., Goodwin, S.F., and Vasconcelos, M.L. (2020). Ovipositor Extrusion Promotes the Transition from Courtship to Copulation and Signals Female Acceptance in Drosophila melanogaster. Curr Biol *30*, 3736-3748.e5. 10.1016/j.cub.2020.06.071.

15. Wang, F., Wang, K., Forknall, N., Parekh, R., and Dickson, B.J. (2020). Circuit and Behavioral Mechanisms of Sexual Rejection by Drosophila Females. Curr Biol *30*, 3749-3760.e3. 10.1016/j.cub.2020.07.083.

16. Klapoetke, N.C., Murata, Y., Kim, S.S., Pulver, S.R., Birdsey-Benson, A., Cho, Y.K., Morimoto, T.K., Chuong, A.S., Carpenter, E.J., Tian, Z., et al. (2014). Independent optical excitation of distinct neural populations. Nat Methods *11*, 338–346. 10.1038/nmeth.2836.

17. Baines, R.A., Uhler, J.P., Thompson, A., Sweeney, S.T., and Bate, M. (2001). Altered electrical properties in Drosophila neurons developing without synaptic transmission. J Neurosci *21*, 1523–1531. 10.1523/JNEUROSCI.21-05-01523.2001.

18. Oren-Suissa, M., Bayer, E.A., and Hobert, O. (2016). Sex-specific pruning of neuronal synapses in Caenorhabditis elegans. Nature *533*, 206–211. 10.1038/nature17977.

19. Lee, G., Hall, J.C., and Park, J.H. (2002). Doublesex gene expression in the central nervous system of Drosophila melanogaster. J Neurogenet *16*, 229–248. 10.1080/01677060216292.

20. Robinett, C.C., Vaughan, A.G., Knapp, J.-M., and Baker, B.S. (2010). Sex and the single cell. II. There is a time and place for sex. PLoS Biol *8*, e1000365. 10.1371/journal.pbio.1000365.

21. Rideout, E.J., Dornan, A.J., Neville, M.C., Eadie, S., and Goodwin, S.F. (2010). Control of sexual differentiation and behavior by the doublesex gene in Drosophila melanogaster. Nat Neurosci *13*, 458–466. 10.1038/nn.2515.

22. Truman, J.W., and Bate, M. (1988). Spatial and temporal patterns of neurogenesis in the central nervous system of Drosophila melanogaster. Dev Biol *125*, 145–157. 10.1016/0012-1606(88)90067-x.

23. Taylor, B.J., and Truman, J.W. (1992). Commitment of abdominal neuroblasts in Drosophila to a male or female fate is dependent on genes of the sex-determining hierarchy. Development *114*, 625–642. 10.1242/dev.114.3.625.

24. Birkholz, O., Rickert, C., Berger, C., Urbach, R., and Technau, G.M. (2013). Neuroblast pattern and identity in the Drosophila tail region and role of doublesex in the survival of sex-specific precursors. Development *140*, 1830–1842. 10.1242/dev.090043.

25. Truman, J.W., and Reiss, S.E. (1976). Dendritic reorganization of an identified motoneuron during metamorphosis of the tobacco hornworm moth. Science *192*, 477–479. 10.1126/science.1257782.

26. Technau, G., and Heisenberg, M. (1982). Neural reorganization during metamorphosis of the corpora pedunculata in Drosophila melanogaster. Nature *295*, 405–407. 10.1038/295405a0.

27. Williams, D.W., and Shepherd, D. (1999). Persistent larval sensory neurons in adult Drosophila melanogaster. J Neurobiol *39*, 275–286.

28. Lee, K., and Doe, C.Q. (2021). A locomotor neural circuit persists and functions similarly in larvae and adult Drosophila. Elife *10*, e69767. 10.7554/eLife.69767.

29. Consoulas, C., Restifo, L.L., and Levine, R.B. (2002). Dendritic remodeling and growth of motoneurons during metamorphosis of Drosophila melanogaster. J Neurosci *22*, 4906–4917. 10.1523/JNEUROSCI.22-12-04906.2002.

30. Sprecher, S.G., and Desplan, C. (2008). Switch of rhodopsin expression in terminally differentiated Drosophila sensory neurons. Nature *454*, 533–537. 10.1038/nature07062.

31. Peng, Q., Chen, J., Su, X., Wang, R., Han, C., and Pan, Y. (2022). The sex determination gene doublesex is required during adulthood to maintain sexual orientation. J Genet Genomics *49*, 165–168. 10.1016/j.jgg.2021.08.006.

Figure 1

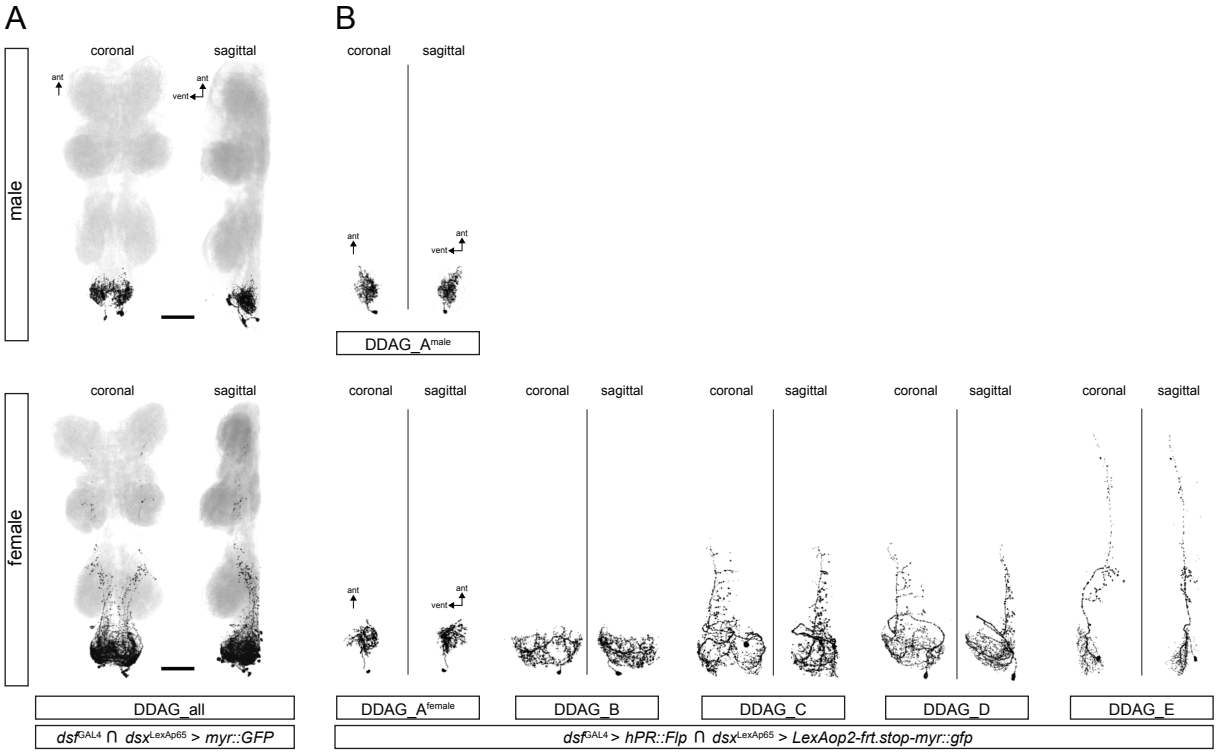
A
B
coronal
sagittal
male
female
ant
vent
DDAG_A^male
DDAG_all
DDAG_A^female
DDAG_B
DDAG_C
DDAG_D
DDAG_E
dsf^GAL4 ∩ dsx^LexAp65 > myr::GFP
dsf^GAL4 > hPR::Flp ∩ dsx^LexAp65 > LexAop2-frt.stop-myr::gfp

Figure 2

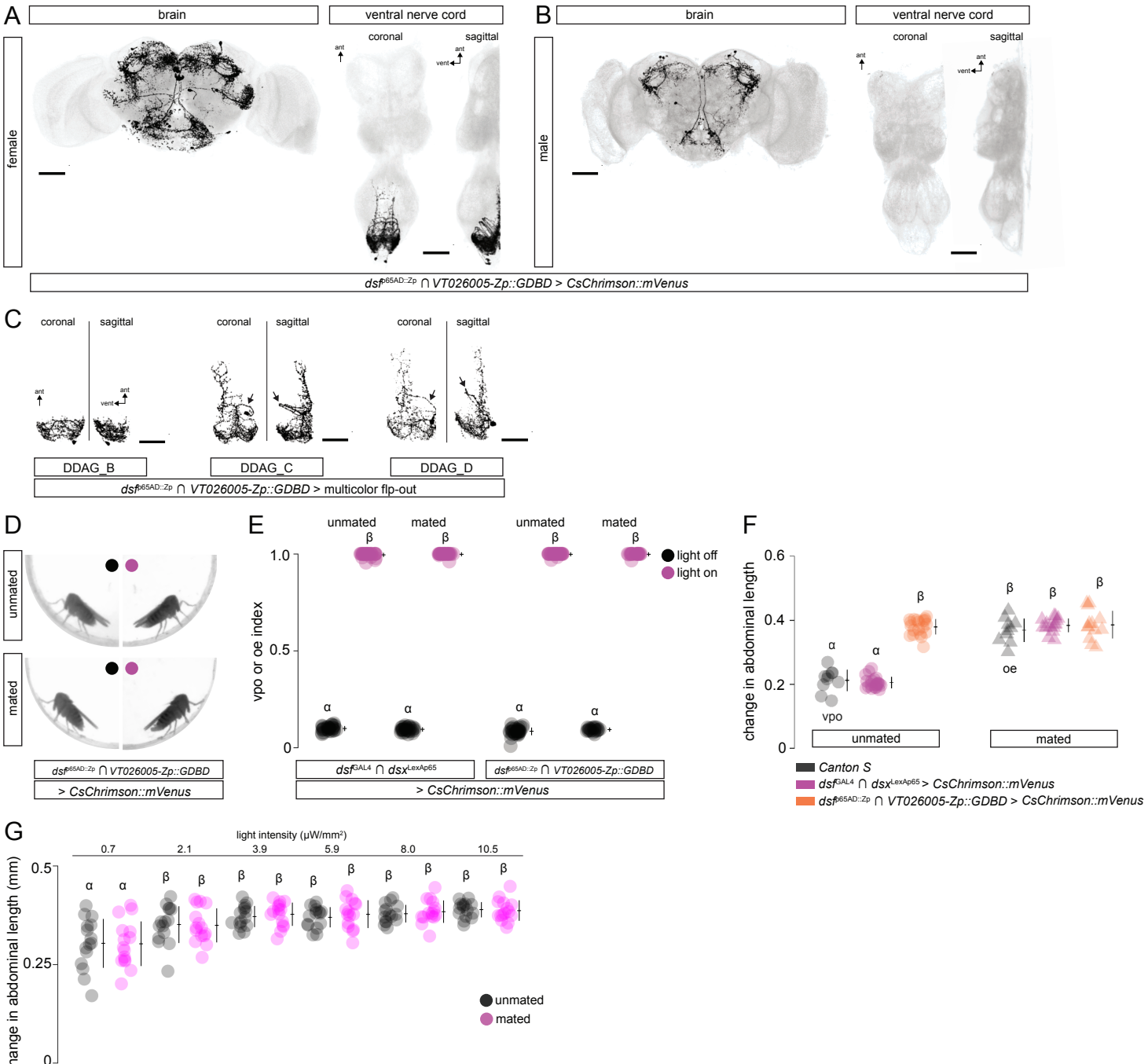
A
brain
ventral nerve cord
coronal
sagittal
female
B
brain
ventral nerve cord
coronal
sagittal
male
dsf^p65AD::Zp ∩ VT026005-Zp::GDBD > CsChrimson::mVenus
C
coronal
sagittal
DDAG_B
DDAG_C
DDAG_D
dsf^p65AD::Zp ∩ VT026005-Zp::GDBD > multicolor flp-out
D
unmated
mated
dsf^p65AD::Zp ∩ VT026005-Zp::GDBD
> CsChrimson::mVenus
E
unmated
mated
light off
light on
vpo or oe index
dsf^GAL4 ∩ dsx^LexAp65
dsf^p65AD::Zp ∩ VT026005-Zp::GDBD
> CsChrimson::mVenus
F
change in abdominal length
vpo
oe
unmated
mated
Canton S
dsf^GAL4 ∩ dsx^LexAp65 > CsChrimson::mVenus
dsf^p65AD::Zp ∩ VT026005-Zp::GDBD > CsChrimson::mVenus
G
light intensity (μW/mm²)
change in abdominal length (mm)
unmated
mated
dsf^p65AD::Zp ∩ VT026005-Zp::GDBD > CsChrimson::mVenus
H
fraction
(n=17) (30) (33) (33) (5) (11) (6)
n/e B C D B C D
unilateral
bilateral
no behavior
postural change
ovipositor extrusion
n=104 unmated females
I
hsFlp, dsf^p65AD::Zp ∩ VT026005-Zp::GDBD > UAS-frt.stop-CsChrimson::mVenus
bilat. DDAG_C
bilat. DDAG_D

Figure 3

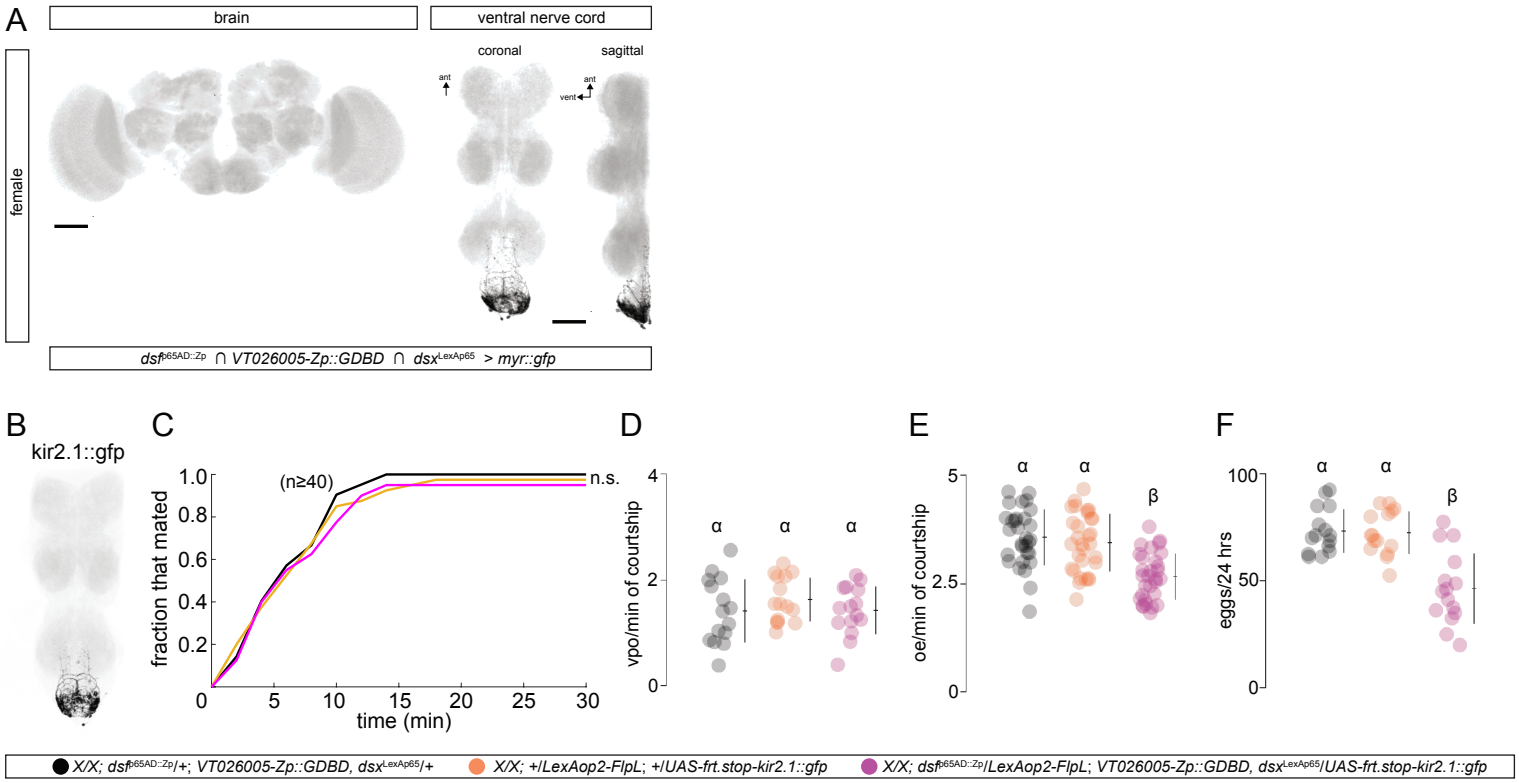
A
brain
ventral nerve cord
coronal
sagittal
ant
vent
ant
female
dsf^p65AD::Zp ∩ VT026005-Zp::GDBD ∩ dsx^LexAp65 > myr::gfp
B
kir2.1::gfp
C
(n≥40)
n.s.
fraction that mated
1.0
0.8
0.6
0.4
0.2
0
5
10
15
20
25
30
time (min)
D
vpo/min of courtship
4
2
0
α
α
α
E
oe/min of courtship
5
2.5
0
α
α
β
F
eggs/24 hrs
100
50
0
α
α
β
X/X; dsf^p65AD::Zp/+; VT026005-Zp::GDBD, dsx^LexAp65/+
X/X; +/LexAop2-FlpL; +/UAS-frt.stop-kir2.1::gfp
X/X; dsf^p65AD::Zp/LexAop2-FlpL; VT026005-Zp::GDBD, dsx^LexAp65/UAS-frt.stop-kir2.1::gfp

Figure 4

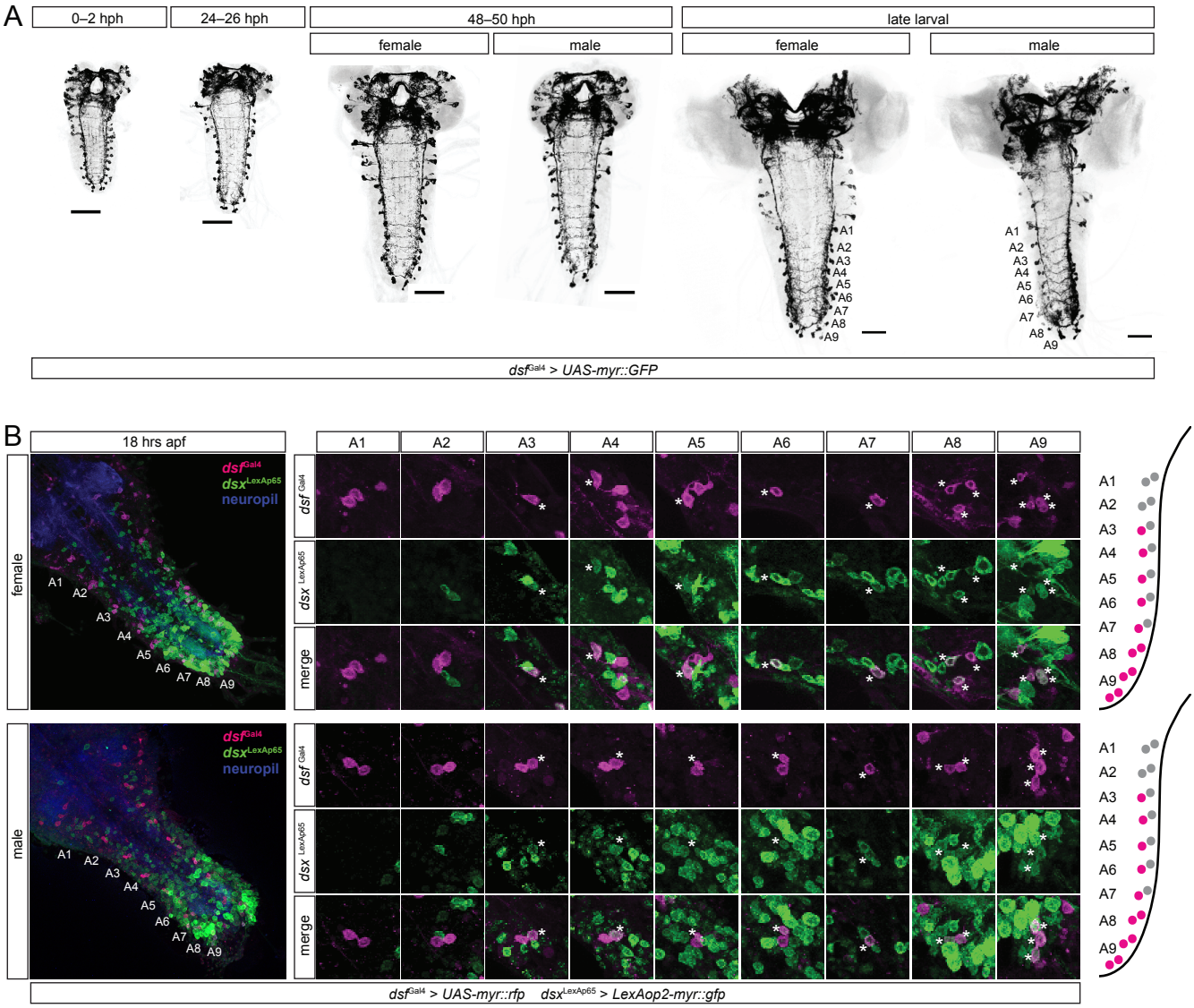
A
0–2 hph
24–26 hph
48–50 hph
late larval
female
male
female
male
A1
A2
A3
A4
A5
A6
A7
A8
A9
dsf^Gal4 > UAS-myr::GFP
B
18 hrs apf
female
male
dsf^Gal4
dsx^LexAp65
neuropil
dsf Gal4
dsx LexAp65
merge
dsf^Gal4 > UAS-myr::rfp dsx^LexAp65 > LexAop2-myr::gfp

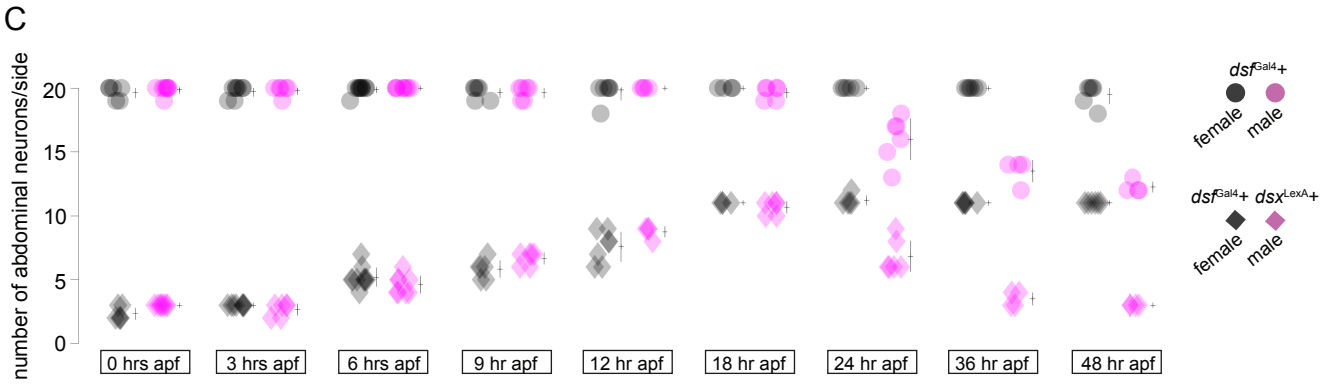
C
number of abdominal neurons/side
20
15
10
5
0
0 hrs apf
3 hrs apf
6 hrs apf
9 hr apf
12 hr apf
18 hr apf
24 hr apf
36 hr apf
48 hr apf
dsf^Gal4+
female
male
dsf^Gal4+ dsx^LexA+
female
male

Figure 5

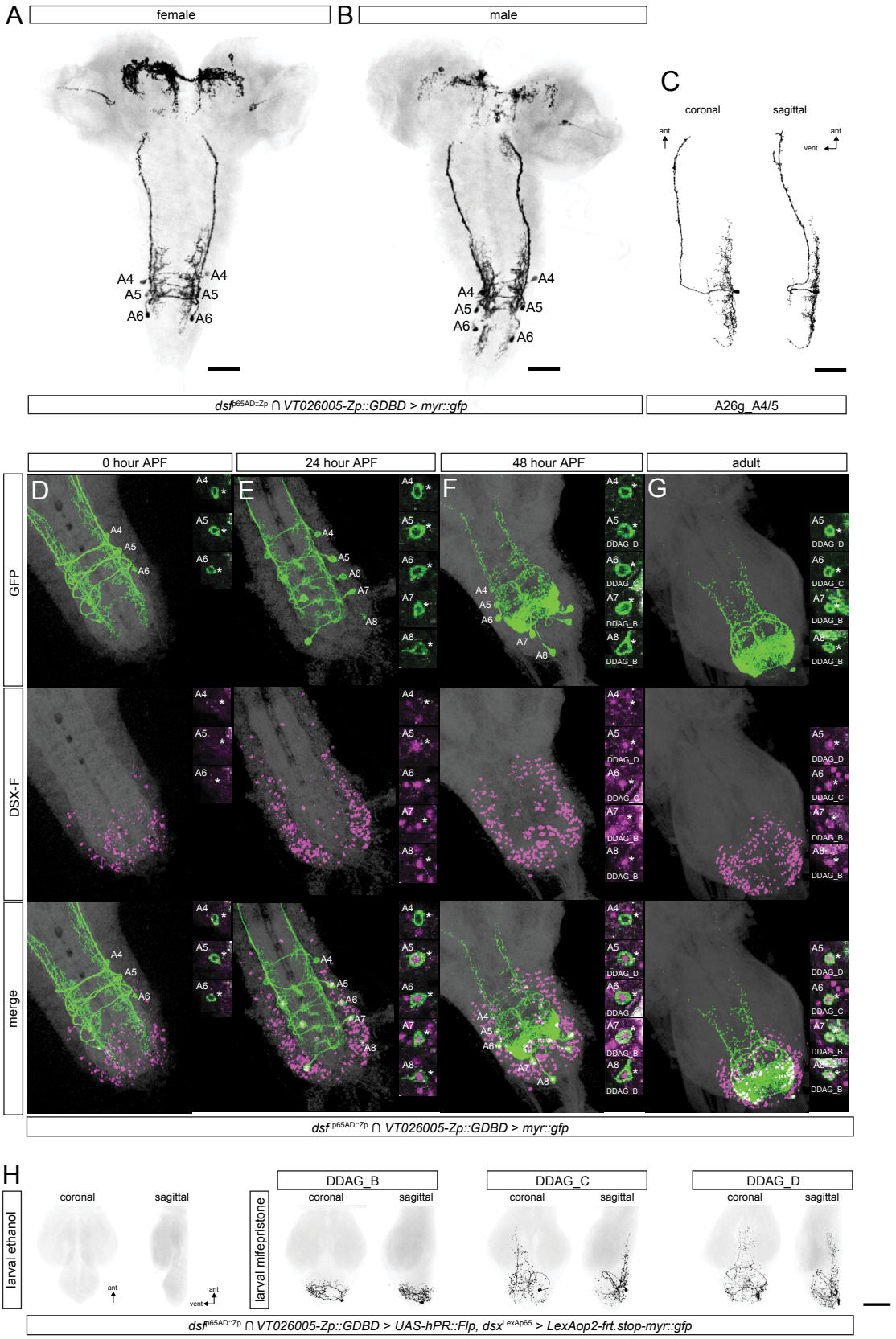
A
female
B
male
C
coronal
sagittal
ant
vent
A4
A5
A6
dsf p65AD::Zp ∩ VT026005-Zp::GDBD > myr::gfp
A26g_A4/5
0 hour APF
24 hour APF
48 hour APF
adult
D
E
F
G
GFP
DSX-F
merge
A7
A8
DDAG_D
DDAG_C
DDAG_B
dsf p65AD::Zp ∩ VT026005-Zp::GDBD > myr::gfp
H
larval ethanol
larval mifepristone
DDAG_B
DDAG_C
DDAG_D
dsf p65AD::Zp ∩ VT026005-Zp::GDBD > UAS-hPR::Flp, dsx LexAp65 > LexAop2-frt.stop-myr::gfp

Figure 6

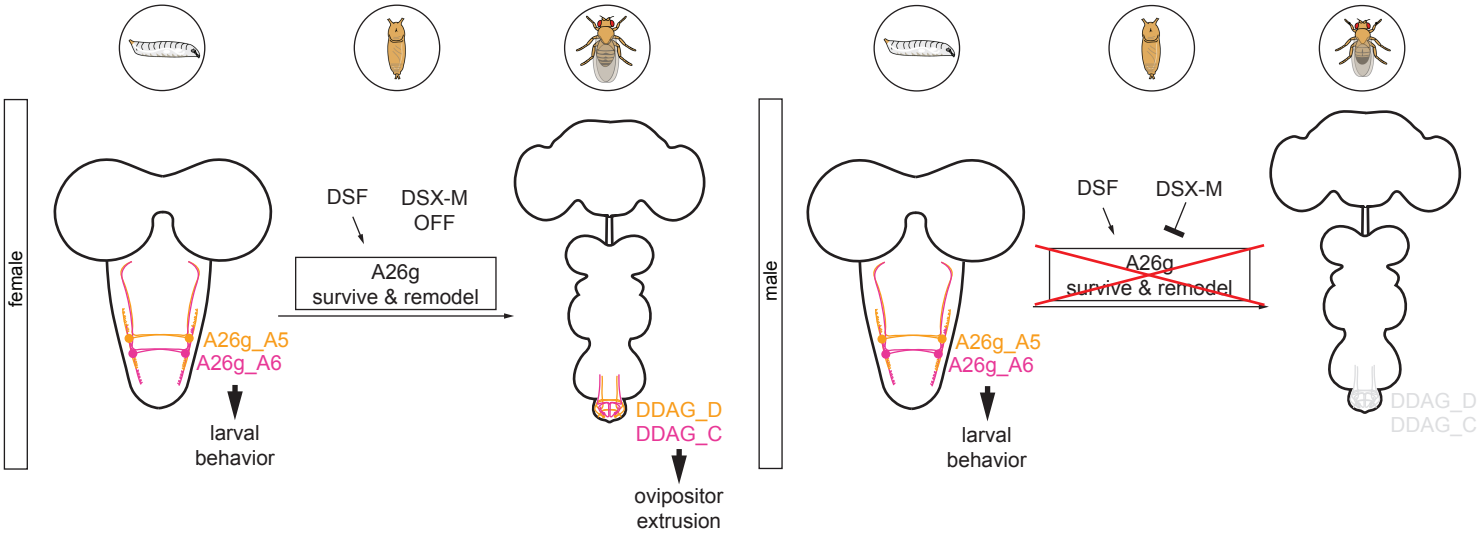
female
A26g_A5
A26g_A6
larval
behavior
DSF
DSX-M
OFF
A26g
survive & remodel
DDAG_D
DDAG_C
ovipositor
extrusion
male
A26g_A5
A26g_A6
larval
behavior
DSF
DSX-M
A26g
survive & remodel
DDAG_D
DDAG_C